Studies on the Process of Development of Alternate Bars

By Yuichiro Fujita and Yoshio Muramoto

(Manuscript received July 22, 1985)

Abstract

Alternate bars play a major role in stream channel processes and are very interesting phenomena in rivers. It has a large influence on the safety of river courses and the use of river water. The mechanism and the process of development of the alternate bar, which may be regarded as one of the most important subjects on the meso scale river bed configuration, are investigated in this paper. One reason for this study is that very few confirmative studies have been carried out by means of detailed experiments. Conducting the experiments under widely changed conditions, particularly that of the channel width, we clarified in detail the characteristic changes of the wave length and the wave height of the alternate bar and the channel bed variations in the development process. The development process of the alternate bar proved to be divided into three phases: in the first phase, the bar edge has become clear and the wave length has almost developed, in the second, the bar increases in the wave height to an equilibrium value and the third is a kind of the equilibrium state of the bar geometry. A longitudinally averaged bed shows a Quonset-hut shaped cross section in the second phase, the height of which increases corresponding to the wave height. This is due to lateral sediment transport caused by the meandering characteristics of flow over the alternate bar. By using the results, we proposed an equation for the development time of the alternate bar, and moreover, experimentally verified the effectiveness of parallel groyne works for the control of the bar geometry.

1. Introduction

Alternate bars are part of the typical river bed configuration of meso scale and one of the most important and interesting phenomena in river mechanics, for they cause scour of river beds and banks alternately and make a river channel unstable by forming a meandering pattern. Even if river banks are stabilized by revetment, as in many rivers in Japan, several kinds of river engineering structures suffer from local scour and deposit due to these bars and not a few are damaged. Many experimental and theoretical studies and some field work have been carried out to clarify their hydraulic characteristics, such as, their formative conditions, geometrical properties and migration velocities. Thus, data have been accumulated from experimental streams and actual rivers. The formative conditions and the geometry of the bar have come to be predictable by dimensional considerations[1]. At the same time, recent stability theories of river bed variation in two dimensional plane have made it possible to give reasonable results of the formative conditions and the wave length of the alternate bar[2,3].

In these stability theories, the formative process of the alternate bar and its mechanism are described by hydraulic equations with various assumptions mainly on the sediment movement. In order to complete the theories, the assumptions as well as the process predicted by the theories must be verified by corroborative investigations. In the previous studies, however, corroborative approaches to the formative process of the alternate bars have been limited solely to descriptions of qualitative observations. Up to the recent years, quantitative and mechanical considerations have never been tried. The process might have first been described by Engels[4] and was not been inferred for quite a long time till Kinoshita[5] reported a detailed but qualitative observation. Similar descriptions were given by Ikeda[6] and Kondo-Komori[7]. They are summarized below, including the authors' observation[8].

(1) Immediately after the flow commencement, sand grains were swept straight downstream, with fluctuating left and right to some small extent.
(2) After a while, obliquely directed lines with very small height appeared here and there on the bed.
(3) The sand grains seemed to be trapped on and under the lines which became a small step with increasing height.
(4) Some of them were seen to turn into clearly distinguished bar edges, increasing their height by sand deposit on the top of the edge and removal from the foot of the edge slope.
(5) These bar edges continued to develop till they reached an equilibrium state.

These observations left the formative process rather vague because any single phase in the process was not confirmed by detailed step by step measurement, but only judged by ostensible observation. Recently, Fukuoka et al.[9] tried to find out governing factors of the early stage of the formative process by means of experiments with some idea on propagation of the sand surface disturbance. In spite of their skillful experiments, it must be said that they were not able to clarify the initial process of the alternate bar formation because of their somewhat overrelience on subjective observations. Thus, the development process of the alternate bar has not yet been made sufficiently clear by corroborative investigations. Though many stability theories have described the mechanisms of the development by using basic equations of fluvial hydraulics while making various kinds of assumptions, these assumptions have hardly been verified by quantitative observations of each step of the process. In almost all theories, moreover, the equations were linearized to eliminate effects of the magnitude of initial disturbances from the results analysed. The validity of the theories were examined only by their final results, such as the wave length and the formative conditions, though the predicted process was not confirmed even in the initial stage of the process. The observed process summarized above suggests that the initial disturbances seen on the bed are much different from those in the theories delineated by the double harmonic complex functions.

The elucidation of this process and its mechanisms not only would verify the validity of assumptions in the stability theories, but also would throw some new lights on the physical meanings of hydraulic parameters of bar formation and the prediction of the deformation under varying flow conditions. Moreover, it will become possible to estimate the wave length and the wave height based on a different standpoint from the stability theories. At the present stage of the investigation, it is most important to observe and grasp the phenomena occurring in the process as much in detail as possible through quantitative measurement.

Standing on the point of view stated above, we have studied the formative process of the alternate bars over these several years, carrying out various kinds of experiments[10–13]. From the results of these studies, characteristic features in the development process is described by the variation of the wave length and height of the alternate bars in the following sections. Conditions of sediment transport in the process is made clear by inspection of variations in the stream bed measured in detail. The mechanism of the bar development is considered in order to present a tentative expression for estimation of the bar development time and to verify the effectiveness of submerged parallel groyne works on reguration of the alternate bar bed. The contents of this paper is that of referrence 10 modified by results from additional experiments conducted subsequently.

2. Experiments on the development process of the alternate bar

2.1 Equipment of experiments

Three flumes of the Ujigawa Hydraulic Laboratory were used in experiments. The first one was an 18 m long, 0.7 m wide, 0.55 m deep concrete flume; the second was a large-sized concrete flume, that is, a 43 m reach of the river course part of the Experimental Facility for Research of River Disaster; and the third was a 20.5 m long, 0.5 m wide, 0.55 cm deep recirculating steel flume with changeable slope. These three flumes are different from each other as will be described below.

In the first flume, as shown in **Fig. 1**, channel widths which varied from 0 to 55 cm and expanding rates between 0 and 23% could be set up by two steel partition walls which were divided into three parts by two hinges. Arranging the steel wall to prescribed channel widths, sand for experiments was carried into it to produce movable bed channels of about 14 m length. Sediment load washed out from the downstream was lead through a guide vane to a submerged trap in a returning flume

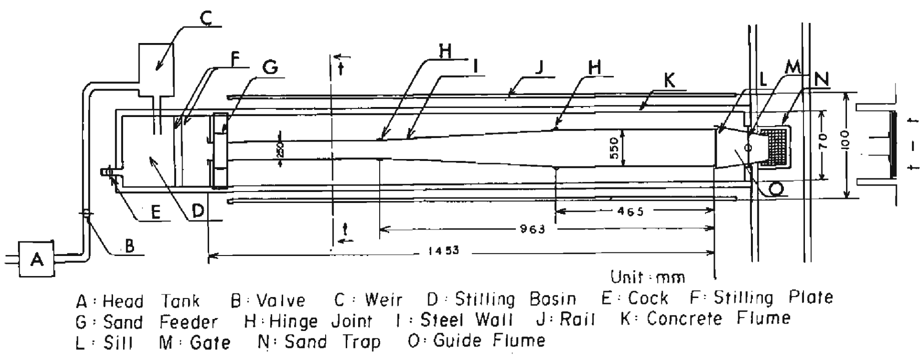

Fig. 1 An experimental flume for runs A–C.

and weighed to determine bed load rates. A rotary sand feeder placed above the inlet could supply sand to 0 to 70 cm width quite uniformly. Two carriages mounted on rails along the flume were used for measurement and for sand surface grading and photographing, respectively. Initial stream beds were formed by a hand-operated grader on the carriage and trowels along slope lines drawn on the walls. Water was supplied from a head tank into the channel and returned to a storage tank while the discharge was adjusted by a valve and determined at a measurement box with a trapezoidal weir placed at the upstream end of the flume. The longitudinal x-coordinate was in the upstream direction and $x=0$ m at the outlet, the lateral y-coordinate was taken from left to right and $y=50$ cm at the center of the channel. The z-coordinate was perpendicular to the x, y-plane and downward.

The second large-sized concrete flume has been introduced already[14]. The present experiments were carried out in a 43 m reach of the indoor part of the flume. The central 2 m width of the 7.5 m wide flume was partitioned along the full length of the reach by plywood for concrete molding boxes to create a 2 m wide, 43 m long fixed wall channel (see **Fig. 2**). About 20 m upstream, the reach from the inlet of the movable bed reach was used as a stilling basin with a capacity more than 100 m^3, while a 5 m downstream reach from the outlet was a settling basin, enclosed by concrete blocks where washed out sediment was trapped to measure transport rates. A sand scraper, a large-sized rotary sand feeder and a measurement carriage were used to form initial beds and take plane pictures, to maintain initial slopes during runs and to measure bed elevations and water surface levels, respectively. All of them are self-propelled along rails laid on the flume walls. Discharge was controlled automatically by a system with an air valve and an electro-magnetic flow meter and determined at a measurement tank with a rectangular weir standing in the stilling basin. Coordinates were taken as follows: x-coordinate was longitudinally downstreamward and $x=80$ m at the inlet, y-coordinate was left-ward and $y=4$ m at the center of the flume, and z-coordinate was perpendicular to the x, y-plane and downward.

The third is a recirculating flume and its 15 m mid reach was glazed. Experimental sand was laid with 8 cm thickness at an 18.4 m reach from the downstream end. A carriage travelled on the side-walls being pull by a variable motor at the upstream

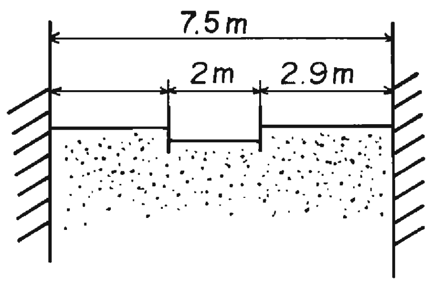

Fig. 2 Schematic sketch of experimental channel cross section in runs D.

end of the flume and was used for measurement, photographing and sand surface grading. Discharge was inspected by a nozzle flow meter attached to the supplying pipe and controlled by a valve during runs to keep the prescribed values. The rotary sand feeder used in the first flume was mounted again at the upstream end of the movable bed and was operated to maintain an intial bed elevation, while at the outlet of the flume, sediment washed out was trapped and weighed in a netted box which was supported by two spring balances and submerged in the tail box. The longitudinal x-coordinate was taken downstream-ward and $x=0$ m at the upstream end of the flume, y-coordinate from right to left and $y=20$ cm at the right side wall, and perpendicular z-coordinate downward.

2.2 Procedures

In every run, the initial bed surface were made as smooth as possible by using the equipment mentioned above. After that, the beds were wetted by a very small discharge in order to be compacted slightly. After their elevations were determined, the flow was released and the sand supply started. In order to measure the bed variations and to pursue the development of the bar geometry during the formative process of the alternate bar, the flow was interrupted 5 to 8 times till the wave length and the wave height kept constant values or began to decrease in their values after the development of the alternate bars attained a kind of equilibrium.

Water stages were measured along three longitudinal lines just before the flow stoppages by either a sand surface detecter switched to water surface mode or a water surface level sensor of a surbo type, which were mounted on the each carriage for measurement. During the stoppage, the bed elevations were measured on 6 to 11 points in each cross section spaced at a longitudinal interval of a half or a third of the channel width, and the bed configuration was sketched to record the planforms of bars. The sediment load trapped in each flow duration was also measured to calculate the transport rates. Plane continuous photographs were taken at short time intervals through the duration and the stoppage of the flow and were used to analyse the wave length and the migration of bars.

2.3 Prescribed conditions and hydraulic quantities

Runs in the present experiments and their prescribed conditions were listed in Table 1, in which runs A to C were conducted in the first, width changeable flume, runs D in the second, large-sized flume and runs H in the third, slope changeable flume. The same sand was used in the first and in the third flume and its grain size accumulation curve is shown in **Fig. 3(a)**. The sand was fairly uniform, the mean diameter, d_m, and $\sqrt{d_{84}/d_{16}}$ of which were 0.99 mm and 1.48, respectively, where suffices denote the percentage of the grain size accumulation curve. **Fig. 3(b)** describes that of the sand used in the second, which was a rather graded sand with $d_m=0.88$ mm and $\sqrt{d_{84}/d_{16}}=2.62$. Such a difference of the grain size distribution did not cause any substantial change in the formative process in the following experiments though a little sorting was discerned in run D–2, for the mean bed shear stress is rather high, such as, nearly or more than twice of the critical one of the mean diameter.

Table 1 Hydraulic conditions in the experiments.

Run No.	Dis-charge Q (l/sec)	Channel width B (cm)	Initial slope	Depth h (cm)	Froude No. F_r	Energy slope I_e	Shear velocity U_* (cm/s)	Flow duration T (min)	T_e (min)
A–1	3.00	55	1/200	1.65	0.84	0.00578	2.9	501	354
A–2	3.00	55	1/100	1.37	1.13	0.01009	3.5	94	—
B–1	1.39	30	1/200	1.50	0.80	0.00659	2.9	309	147
B–2	1.43	30	1/100	1.36	0.96	0.01508	3.5	136	55
C–1	3.00	40	1/100	1.77	1.09	0.009475	3.8	98	44
C–2	1.95	40	1/100	1.26	1.13	0.009347	3.2	162	66
D–1	43.78	200	1/300	4.15	0.84	0.003507	3.6	366	270
D–2	43.78	200	1/200	4.32	0.79	0.002592	3.1	560	560
H–1	1.90	50	1/200	1.36	0.77	0.00543	2.62	61.5	—
H–2	4.02	50	1/200	2.11	0.84	0.00557	3.26	330	200
H–3	5.6	50	1/100	2.06	1.23	0.00962	4.24	73	73

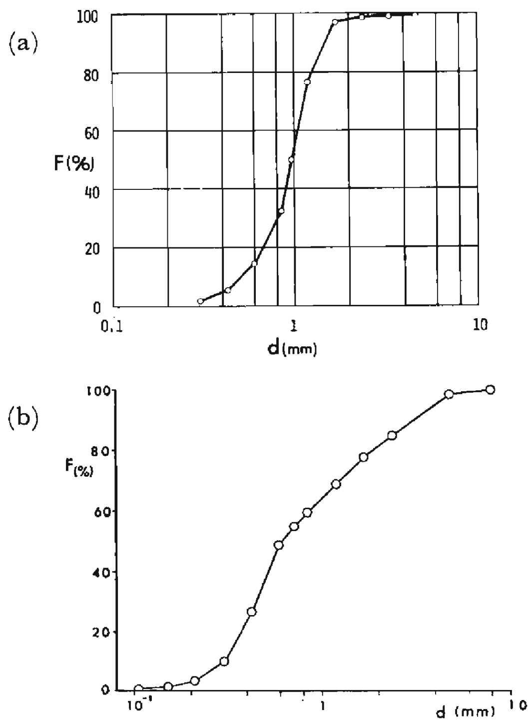

Fig. 3 Grain size accumulation curves of the sand used; in runs A, B, C and H: (a) and in runs D: (b).

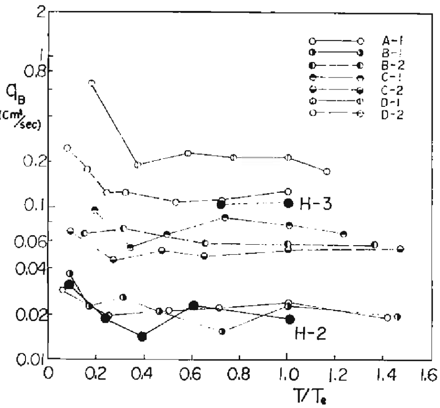

Fig. 4 Changes of bed load rates per unit width measured at the downstream ends.

The hydraulic conditions were determined to be included within the mid region of the alternate bar formation on a criterion diagram proposed by the authors[1] for the river bed configuration of meso scale. Channel widths were changed rather widely by using the three flumes to consider scale effects of the experiments.

Hydraulic quantities of the cross sectional mean computed from the averaged water stage and the bed level proved to vary little in the longitudinal direction. Their longitudinally averaged values also had very small changes with time. The averaged hydraulic quantities at the final states are listed in **Table 1**.

Changes of the bed load rates per unit width at the outlet proved to be included in the range of the previous experimental values when they were compared with Ashida-Michiue's bed load function. Their change with time are listed in **Table 2** and depicted in **Fig. 4** with a dimensionless time by a development time, T_e, that is, a time required by the development of the alternate bar defined later. In almost all runs, the rate kept constant values corresponding to the very small variation of the hydraulic quantities though those in the early stage were a little larger. Thus, the development of the alternate bar scarcely affects the averaged state of the longitudinal bed load transport since the larger values in the early stage can be attributed mainly to the influence of the initial bed smoothing.

3. Development process of the alternate bar

3.1 Characteristic features of the development process

Variations of the bed forms in the development process were recorded in the plane pictures in almost all runs. Additionally, dimensions of the bed forms were measured minutely in some runs. Characteristic features of the bar behaviors are stated here according to the measured data as well as pictures.

Fig. 5 illustrates the bedform variation in the development process observed in

Table 2 Changes with time of sediment load, wave lengths and wave heights of bars.

Run No.	Time	Sediment load per unit width at the outlet	The bar geometry in the inspection reach		The longitudinally averaged reach		The bar geometry in the averaged reach		Remarks on bedforms
					from	to			
	T	q_B (cm²/sec)	l_B (m)	Z_B (cm)	x (m)	x (m)	l_B (m)	Z_B (cm)	
A–1	21′	0.0284	1.68	1.48	−0.3	11.0	1.68	0.93	discontinuous
	83′	0.0195	1.71	2.39	0.3	10.50	1.71	1.58	
	161′	0.0210	1.92	3.95	0.8	9.02	1.99	3.76	
	250′	0.0219	2.73	3.91	0.04	7.77	2.58	4.18	
	354′	0.0238	1.94	3.47	0.55	8.30	2.15	4.32	
	501′	0.0191	1.25	2.95					
	average	0.0223							
A–2	35′	0.0770	1.56	2.89	0.85	6.55	1.41	1.87	
	70′	0.0834	1.48	2.35	−0.2	7.10	1.83	2.89	
	94′	0.0724	1.93	3.39	0.05	6.60	2.25	3.83	
B–1	13′	0.0363	0.66	0.44	0.20	4.60	0.66	0.44	
	25′	0.0225	0.83	0.58	0.25	3.00	0.88	0.70	discontinous
	46′	0.0257	1.35	0.70	0.20	6.85	1.61	0.80	complicated
	67′	0.0208	0.93	0.62	−0.10	6.75	1.02	1.01	ditto
	106′	0.0155	1.04	1.03	−0.20	6.93	1.19	1.33	regular
	147′	0.0230	1.14	1.35	−0.10	6.88	1.40	1.51	ditto
	228′	0.0195	1.10	1.33	−0.10	7.82	1.51	1.26	
	309′	0.0200	1.97	1.77	0.20	6.58	2.16	1.65	
	average	0.0210							
B–2	8′	0.0673	0.85	0.42	0	7.12	0.79	0.40	
	17′	0.0730	1.14	0.80	0.45	7.52	1.18	0.72	
	36′	0.0585	1.20	1.59	0.05	6.68	1.22	1.38	
	55′	0.0585	1.27	2.11	−0.30	7.42	1.52	2.11	
	74′	0.0585	1.10	1.89	0.59	7.07	1.08	2.00	
	96′	0.0520	1.61	1.92	1.00	7.50	1.63	1.99	
	116′	0.0572	1.20	1.58	1.02	7.13	1.22	1.52	
	136′	0.0589	1.19	1.29	0.65	7.58	1.16	1.25	
	average	0.0605							
C–1	8′	0.0953	0.93	0.92	0.55	5.96	0.90	0.89	
	15′	0.0545	1.02	1.10	0.03	5.87	1.17	1.34	
	21′	0.0665	1.12	1.04	1.09	4.96	0.96	1.00	
	32′	0.0868	1.43	1.83	0.56	5.12	1.52	1.95	
	44′	0.0785	1.24	1.51	0.48	6.97	1.62	2.45	
	54′	0.0687	1.35	2.23	0.64	4.68	1.35	2.23	
	74′	0.0717	1.20	1.28	0.10	5.48	1.35	1.75	
	98′	0.0724	1.34	0.90	0.23	5.62	1.30	0.85	discontinuous
	average	0.0743							

(Table 2 continued)

Run No.	Time T	Sediment load per unit width at the outlet q_B (cm²/sec)	The bar geometry in the inspection reach l_B (m)	Z_B (cm)	The longitudinally averaged reach from x (m)	to x (m)	The bar geometry in the averaged reach l_B (m)	Z_B (cm)	Remarks on bedforms
C–2	6′	0.0686	1.07	0.66	0.20	5.24	1.26	0.91	
	18′	0.0457	1.53	1.58	0.13	6.28	1.54	2.00	
	31′	0.0522	1.34	2.11	0.32	6.45	1.53	2.39	
	43′	0.0482	1.39	2.13	1.04	6.05	1.67	2.63	
	66′	0.0536	1.77	2.40	0.85	7.02	2.06	2.97	
	97′	0.0548	1.41	2.01	0.88	5.40	1.54	2.58	
	162′	0.0565	1.45	1.99	0.08	7.33	1.45	1.99	
	average	0.0540							
D–1	48′						2.43	0.90	
	99′	0.193			92.0	121.3	5.24	1.25	
	156′	0.233			90.2	122.1	5.96	2.63	
	208′	0.217			89.2	122.4	8.30	3.94	
	270′	0.218			91.2	119.3	9.36	7.35	
	320′	0.179			93.5	123.0	9.83	7.15	
	366′	0.220			96.7	116.7	10.50	7.10	
	average	0.210							
D–2	47′	0.246			80.0	91.4	1.90	1.43	
	90′	0.179			84.3	97.8	4.20	1.75	
	132′	0.125			85.2	106.1	4.45	2.13	
	178′	0.126			85.6	111.9	7.05	2.33	
	295′	0.109				118.7	10.27	4.85	
	403′	0.112			88.5	123.3	11.60	5.62	
	560′	0.129			84.2	118.4	10.03	5.90	
	average	0.130							
H–2	17′45″	0.031	0.80	0.25			1.10*	0.40*	
	45′23″	0.018	1.00	0.34			1.33*	0.56*	
	76′50″	0.014	1.43	0.77			2.00*	1.30*	
	120′	0.023	1.66	1.56			2.30*	2.54*	* averaged bar geometry within the 4th maximum height.
	200′	0.019	1.62	1.86			2.13*	3.06*	
	330′	0.022	1.91	1.79			2.50*	2.86*	
	average	0.021							
H–3	9′		0.74	0.32			0.83*	0.66*	
	23′		1.86	1.63			2.15*	2.04*	
	52′30″	0.103	2.23	2.16			2.28*	2.71*	
	73′	0.111	2.80	2.06			2.23*	2.98*	
	average	0.107							

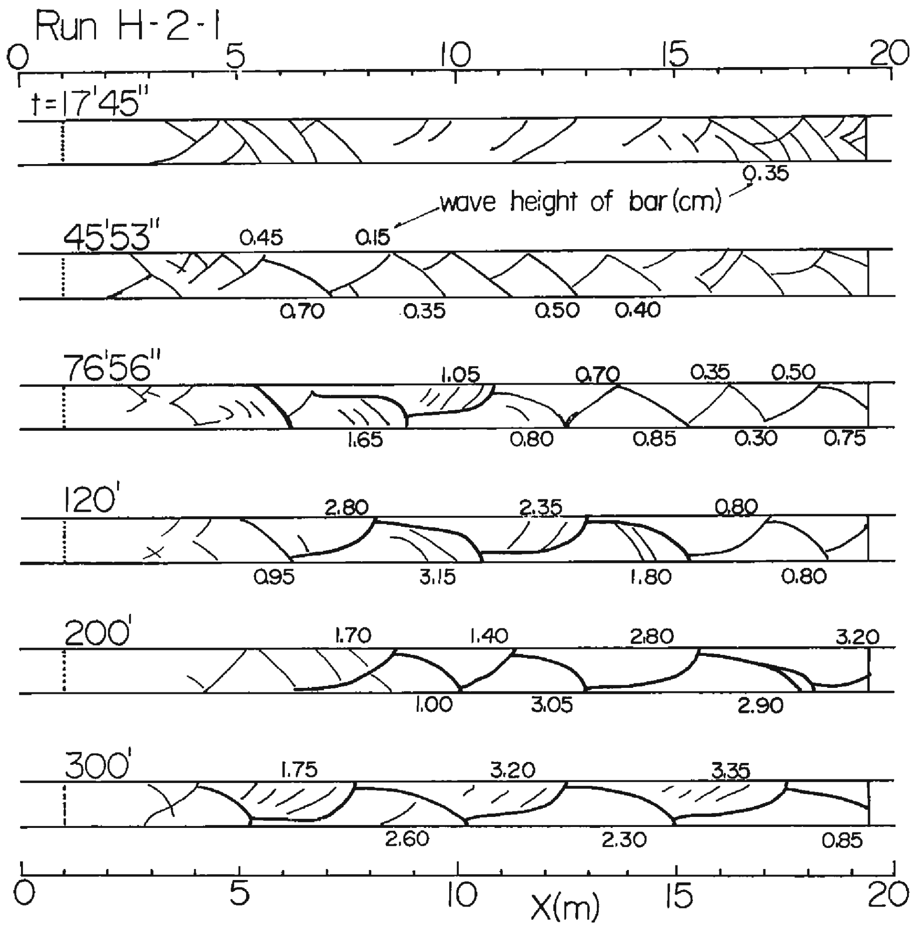

Fig. 5 Variations of bedforms in run H–2.

run H–2, which is an example of the detailed measurement of the bed configuration. As soon as the flow started, oblique stripe patterns covered the whole stream bed. Then fairly prominent lines remained on the dry bed at the first flow stoppage of $t=17'45''$. But the bedform recognized as the bar edge was found only at the most downstream reach and there was no joining state of the alternate bar to determine the wave length. At $t=45'53''$, bars with small wave heights lined up alternately in a 10 m reach from $x=5$ m to $x=15$ m and the wave lengths were easily defined. As shown in the sketches at $t=45'53''$ and at $t=76'56''$, the wave heights have a decreasing tendency in the downstream direction starting from the most developed bar in the development process. A most rapidly developing bar is presumed to make another bar form and develop easily, which is faced alternate side in the immediately downstream reach. The same decreasing tendency of the wave height was affirmed in other runs from variations of the longitudinal profiles of the stream bed.

Thus, the bars hardly develop uniformly along the whole reach of the stream bed, unlike the premise of the stability theories, and a bar developed rapidly due to some causes propagates new bars downstream one by one just like a chain-reaction. This propagation process implies an increase in the wave lengths with time[18] and mutual interference between the first propagating series and the second ones originating more downstream. Another phenomenon occurs when poorly-developed bars which come from the upstream reach onto a distinctive bar seem to be absorbed and then disappear. Therefore, when a rapidly developed bar fortunately occurs at a rather upstream reach of the experimental flume, as in run H–2, a simple, neat diagram of bar migration can be obtained in the development process. In contrast, **Fig. 6** describes a migration diagram in run C–2 where the several rapidly developed bars formed fairly uniformly in a rather downstream reach from the early stage. Curves in **Fig. 6** show a somewhat complicated bar behavior in the middle $x=5$ to 9 m reach due to the mutual interference pointed out above. In such a case, the wave heights have an indiscernible tendency of longitudinally decreasing.

The appearance of these rapidly developing bars are dependent on the conditions of the initial bed, the inlet flow and the sand supply. If the initial bed has some irregularity or nonhomogeneity, bar formation nearby is either hastened or retarded. The former case was observed in run C–2 while the latter was presumed to occur in runs D where the initial bed had a lateral inclination of about 1/250 as a

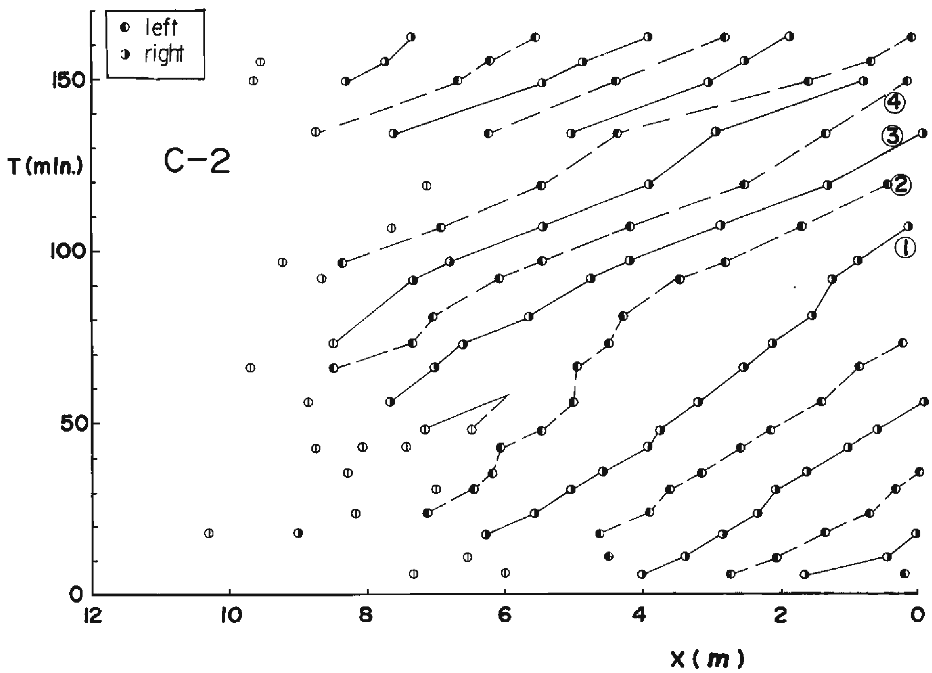

Fig. 6 The diagram of bar migration in run C–2.

mean due to a rail error, and then it took more than 100 minutes for the first bar to appear. Since uniformity of both the inlet flow and the sand supply continues to maintain the conditions of the upmost stream reaches similar to the initial state, it makes bars hard to develop promptly there. Under such conditions, bars seem to form only by accidents of the sand transportation as well as the case under a much smoothened initial bed condition.

3.2 Variations of the wave length and the wave height in the development process

In a reach downstream 5 times the length of the channel width away from the inlet, disturbances due to the inflow and to the sand supply seemed to disappear and bars were found almost always after a certain time. The reach was defined as an inspection reach of variations of the wave length and the wave height in the development process. They were an $x=0$ to 10 m reach in runs A–C, an $x=90$ to 123 m in runs D and an $x=5$ to 20 m in runs H. The wave lengths examined here were average values of l_B measured in the inspection reach, where l_B was defined as a bar edge length orthogonally projected to the x-axes and corresponded to a half of the wave length of the flow meander. The wave height, Z_B, was defined in each cross section as the maximum difference of bed elevation with the bar edge between. The wave height of a bar, Z_{Bmax}, was also defined as the maximum value of Z_B at that bar reach and averaged values of Z_{Bmax} in the inspection reach, $\bar{Z}_{Bmax}$, were used here. For the simplicity overbars and subscript $_{(max)}$ are omitted below.

Changes of l_B and Z_B at the inspection reaches and those at reaches where longitudinally averaged cross sections were calculated, which will be explained in **4.2**, are listed in **Table 2**. The values in the latter reaches will be used in the following examinations and their changes have been demonstrated with time in **Fig. 7**. In runs A–C and H, curves of l_B gather rather closely together and their maximum values appear rather early than those of Z_B. It suggests that increase in the wave heights were accelerated after the wave lengths were almost determined. In runs D, though l_B and Z_B reach their maximum value simultaneously, Z_B begins a rapid increase after $T=200'$ when l_B becomes about 9 m, 70–80% of the maximum values in the both runs D–1 and 2. The results in runs D are essentially consistent with those in runs A–C and H, so it has been concluded that the wave heights begin to increase prominently after the wave lengths are almost determined, taking into accounts that the wave lengths fluctuate easily according to the differences of the migration velocities.

Anomalously, the values of l_B and Z_B of runs H are much smaller than those of runs A–C in spite of being nearly the same scale of experiments. This anomaly is ascribed to the minute measurement of the bed form in runs H: as the main aim of the runs H is to elucidate the origin of the alternate bar and the initial stage of the development process, small bed forms like the oblique lines were measured from the initial state to the final one, even those discerned on the developed bars and all of these dimensions were reflected in the mean values plotted in the **Fig. 7**.

At a considerable time later, new, poorly-developed bars traveled downstream into the inspection reach and affected the values of l_B and Z_B. In order to examine their influences, similar changes of l_B and Z_B of individual bars are also depicted in

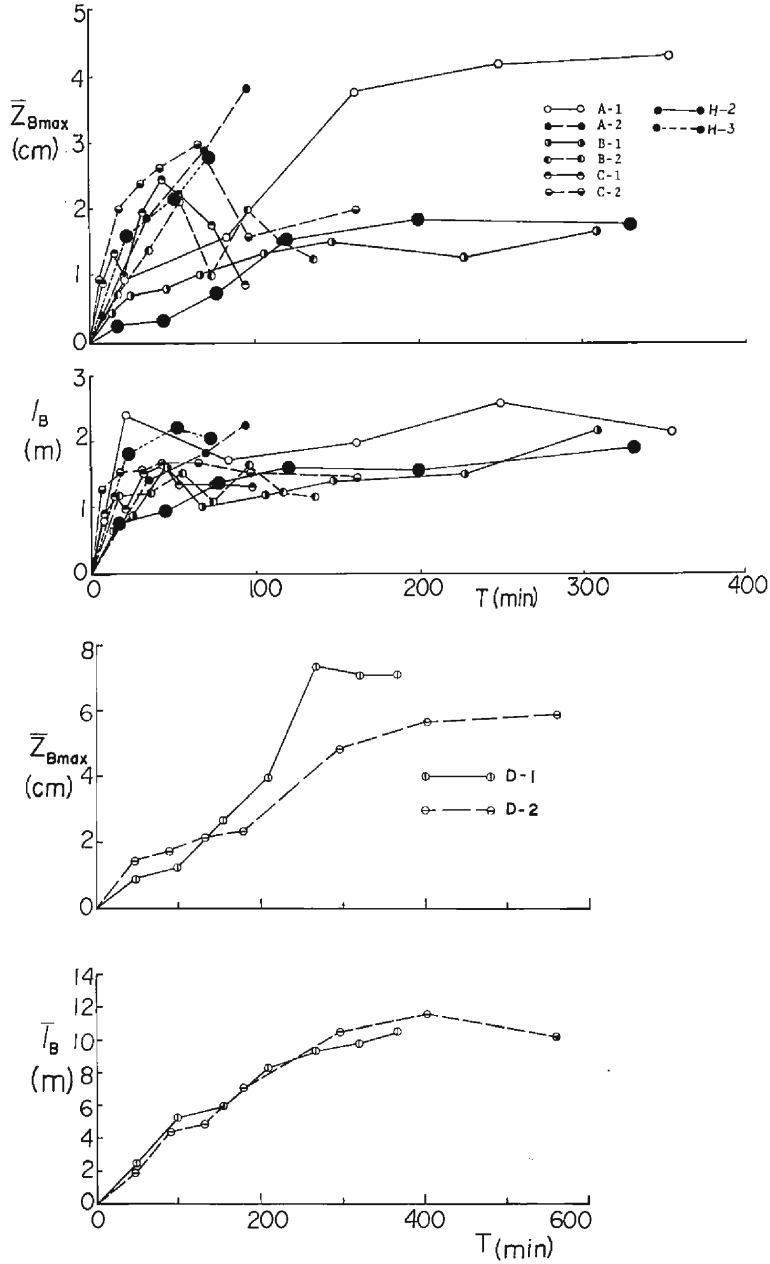

Fig. 7 Development of the wave length and the wave height of the alternate bars.

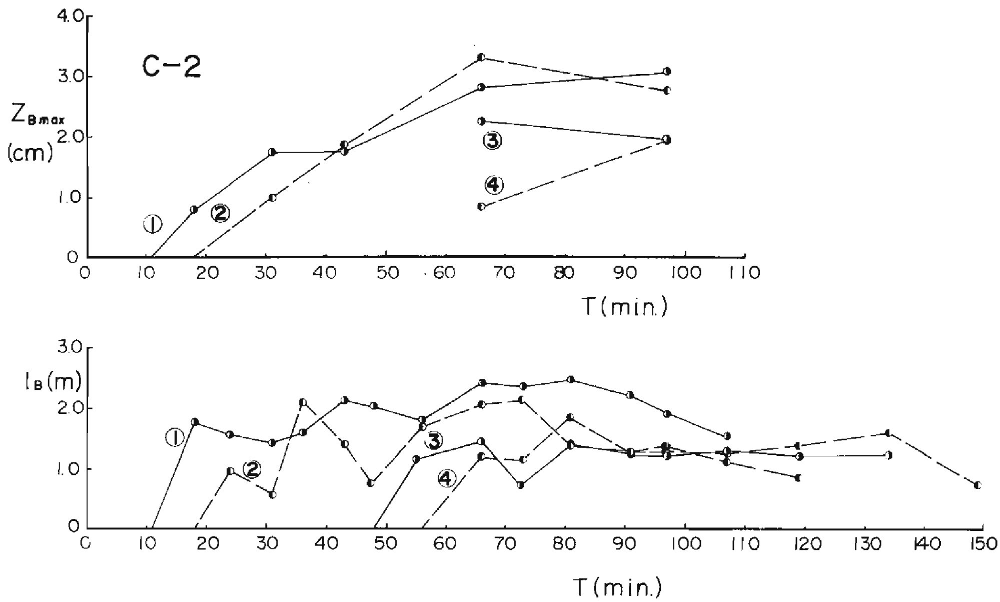

Fig. 8 Development of the wave length and the wave height of individual alternate bars.

Fig. 8, in which circled numbers coinsides to those in **Fig. 6**. There also is a fairly clear tendency of Z_Bs' development after l_Bs' determination, as described especially by the curves of ①, though the wave length curve of ② shows a quite large fluctuation. This fluctuation occured when a bar traveling from the upstream reach was absorbed into the ② bar and disappeared. This leads potentially to misunderstanding of the characteristic feature of the whole development process.

The above variations of the wave lengths and wave heights suggest that development time of the alternate bar is adequately defined as the time at which the wave height, Z_B, attains its first maximum value. The development time, T_e, in each run is listed in **Table 1**, too. Here, the equilibrium values of l_B and Z_B are also defined as those at $T=T_e$ and expressed as l_{Be} and Z_{Be}, respectively. The maximum values of l_B and Z_B proved to be included in the same range of the previous experimental values[1], being compared in the nondimensional form by the channel width, B. It implies that the previous results corresponded to the fully-developed alternate bar.

3.3 Phases dividing the development process of the alternate bar

For the purpose of the more minute inspection of the difference in the development process among the experiments, variations of the wave lengths and the wave heights non-dimensionalized by their equilibrium values, l_B/l_{Be} and Z_B/Z_{Be}, respectively are depicted with a similar dimensionless time T/T_e in **Fig. 9** and a relationship between l_B/l_{Be} and Z_B/Z_{Be} in **Fig. 10**. As both curves of l_B/l_{Be} and Z_B/Z_{Be} to T/T_e differ from each other, the development process with time is not similar but subject to the experi-

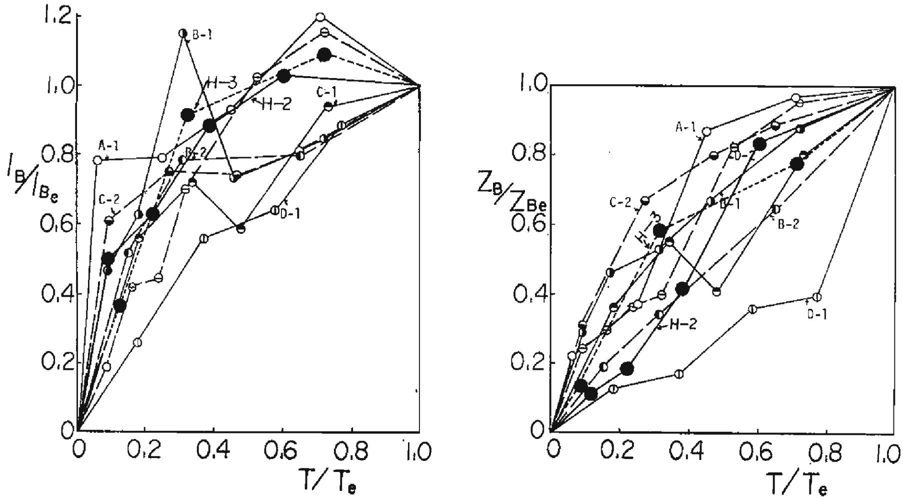

Fig. 9 Development of the wave length and the wave height in a nondimensional form.

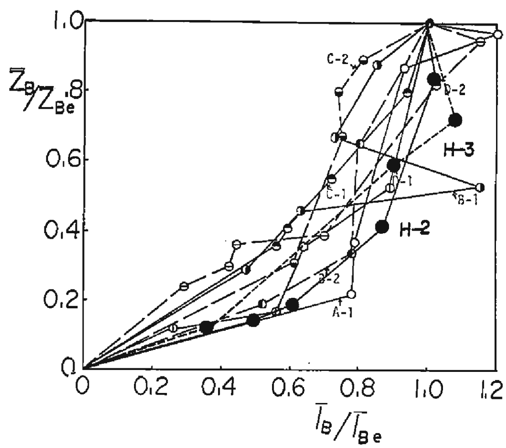

Fig. 10 A nondimensional relationship between the wave length and the wave height in the development process.

mental conditions for the equilibrium values of the wave length and the wave height as well as the development time. On the other hand, curves depicting the bar development in **Fig. 10** gather fairly closely together on account of the broad experimental conditions, and all curves have an upward concave shape, showing that large increases in Z_B/Z_{Be} are more than 60% of the total amount in a range such that $l_B/l_{Be}>0.6$. The curves suggest further the rapid increase in wave height after the almost complete determination of the wave length. At the instance that $l_B/l_{Be}=0.6$, the experimental observation and the pictures show that the bars began to have distinctive edges with regular alternation.

According to such distinctive features of the development process, the whole process can be divided into the following three phases, illustrated schematically in **Fig. 11**.

(1) The first phase: The bar edges become conspicuous and then the wave length increases more rapidly than the wave height. This phase finishes when the wave length ceases its rapid increase.

(2) The second phase: The wave height maintains a rapid increase while the wave length fluctuates slowly near a constant value after a mild increase. This phase continues till the wave height takes the first maximum value. Most of the development time is taken during this phase.

(3) The third phase: This is a kind of the equilibrium state of the bar development, and the wave length and the wave height fluctuate near the constant (equilibrium) values slowly.

Now, defining tentatively the first and the second stages to be divided at the time when the values of l_B/l_{Be} become 0.6, the values of t_e/T_e are found to have a wide range of 0.04 to 0.47 from **Fig. 9**, where t_e is a time when the first phase finished. The wide range of t_e/T_e is ascribed to the rather wide experimental conditions. Thus, the differences in the development process are expressed mainly by the values of both t_e/T_e and Z_{Be}'/Z_{Be}, where Z_{Be}' is the wave height when $T=t_e$. Characteristics of Z_{Be}' are examined here by using data in **Table 3** obtained from **Fig. 9** and **10.** Presumably, Z_{Be}' is proportional to the grain size of the bed material, d, by a factor β, then

$$Z_{Be}'=\beta d. \tag{1}$$

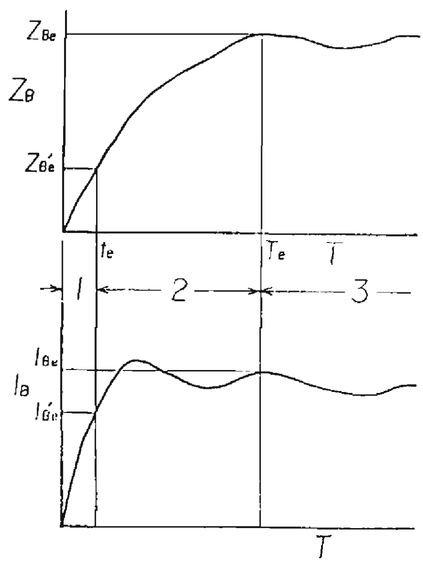

Fig. 11 A schematic sketch of the three phases of the development process of the alternate bar.

Moreover Z_{Be}' is considered to increase with the channel width, B, and in the early stage, the process is governed mainly by factors concerning the bed conditions only,

$$Z_{Be}'/d = \text{fn}(B/d). \tag{2}$$

The relationship between Z_{Be}'/d and B/d is shown in **Fig. 12** and a clear empirical equation is obtained by eye, though the number of the points is small.

$$Z_{Be}'/d = 0.15(B/d)^{2/3}. \tag{3}$$

These findings suggest that hydraulic mechanisms governing the development process differ from each other between the first and the second phases. In the first,

Table 3 The wave height characteristics at the end of the first phase of the alternate bar development.

Run No.	B (cm)	d (mm)	Z_{Be} (cm)	Z_{Be}' (cm)	Z_{Be}'/Z_{Be}	t_e/T_e	Z_{Be}'/d	B/d
A–1	55	0.99	4.32	0.73	0.17	0.04	7.3	556
B–1	30	0.99	1.51	0.65	0.43	0.16	6.5	303
B–2	30	0.99	2.11	0.49	0.23	0.20	4.9	303
C–1	40	0.99	2.45	0.99	0.41	0.22	10.0	404
C–2	40	0.99	2.97	0.89	0.30	0.09	8.9	404
D–1	200	0.88	7.35	1.91	0.26	0.47	21.7	2270
D–2	200	0.88	5.90	2.24	0.38	0.29	25.5	2270

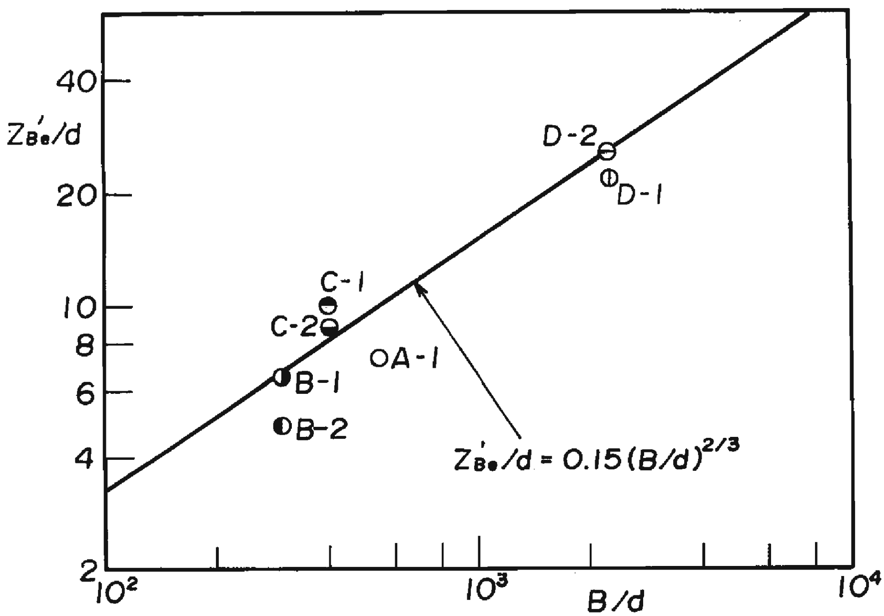

Fig. 12 The wave height at the end of the first phase of the development process.

main roles are presumably played by integrating phenomena of the underdeveloped bedforms such as the semi bar[1]. On the other hand, the wave height increases according to a state of sediment transport due to the flow characteristics ruled by the bed topography of the developing alternate bar. The increasing portion of the wave height during the second stage occupies more than 60% of the total height. As pointed out already, this phase consumes more than 70% of the development time in almost all runs. Furthermore, the wave height of the alternate bar is a main factor governing the flow meandering intensity[15] and the local scouring severity. Therefore, considering the serious and rather accidental effects of the initial and the upstream boundary conditions in the first phase, the development process in the second phase is regarded as representing the whole development process, comprehensively. Practically, it is of high importance in river engineering to investigate the mechanism of the alternate bar development in the second phase, because the mechanism is the very cause of the local scour around the river structures, such as bridge piers, bank revetments and so on.

4. The mechanism of the alternate bar development

4.1 Stream bed variations with the alternate bar development

An actual state of stream bed variations in the development process of the alternate bar has been inspected, as an example, by using accurate data on the bed elevation measurement in run C–2.

Figs. 13 and **14** show longitudinal bed profiles along the centerlines and the both side-walls and the contours of the bed elevation, respectively above a base plane which is defined by a regression plane of the mean bed elevations of the cross sections at each flow stoppage. In **Fig. 13**, the bed profiles mingle with each other and the center profile runs between the both side-wall profiles till $T=6'$. When $T=18'$, the center profile coincides to both side-wall profiles in parts upper than their intersecting points. Then it turns to envelop the uppermost parts of the both side-wall profiles after $T=31'$, while alternately eroded parts of both side-wall profiles become more and more conspicuous in a reach lower than $x=7$ m though the their profiles present rather flat V-shape in this stage. In the other reach upper than $x=7$ m, the profiles show nearly the same state as that at $T=6'$. At $T=66'$, which is regarded as the development time, the eroded parts become greater and turn into U-shape in an $x=0$–9 m reach, with little change of the center profile. Moreover, when $T=97'$ the largely eroded parts migrate downstream and new underdeveloped bars, similar to those at $T=6$–$18'$, travel from the upper reach and occupy more than a half of the inspection reach.

As shown also in **Fig. 13**, the development process of several bars in the inspection reach is fairly uniform in run C–2. But such a uniform process is rather different from those observed in the other runs where the bar development propagated downstream came from a prominent upstream bar, which has already been pointed out in

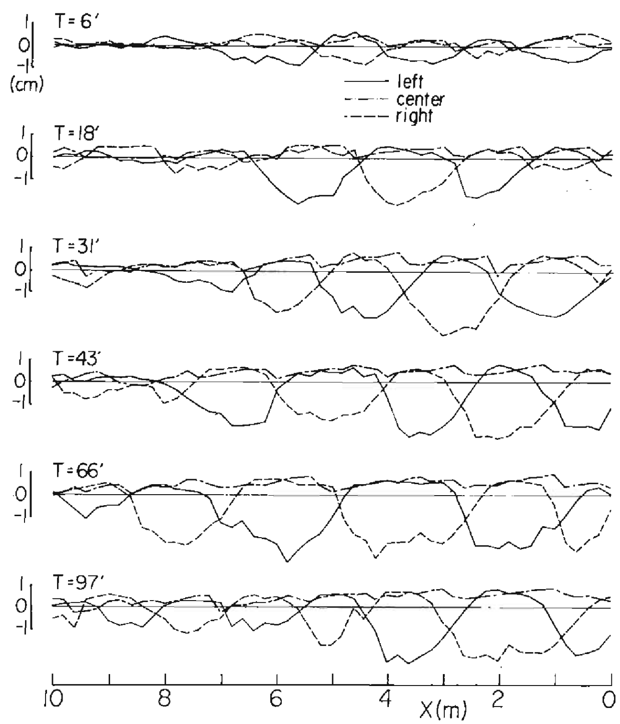

Fig. 13 Bed variations along the centerline and the both side-walls corresponding to the alternate bar development.

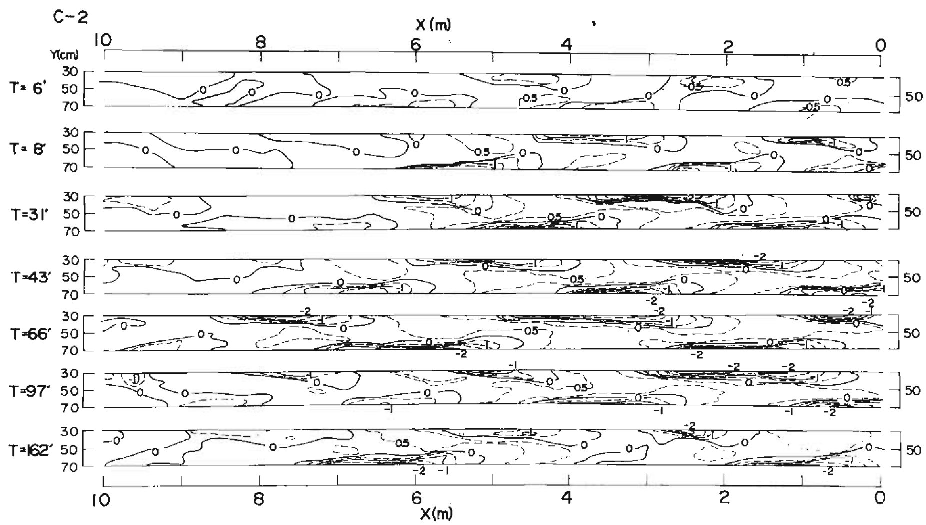

Fig. 14 Variation of the bed topography corresponding to the alternate bar development.

the explanation of **Fig. 5** of run H–2. In such cases, the eroded parts of the bed profiles become smaller one by one in the downstream direction. The uniform development in run C–2 is attributed to the initial bed condition, which is assumed to have some periodical disturbance of not only the elevation but also the porosity of the bed, for the initial bed arrangement by manual trowels presumably did not remove some trace of the antecedent run C–1 thoroughly.

Next, in **Fig. 14**, differences of the bed elevation at $T=6'$ are small and upper and lower zones than the base plane, which is a regression plane of the bed and is expressed by 0 cm contours, cut across the channel central region by turns. Then at $T=18'$ the central region is covered with the deposition zones and contours of 0.5 cm are going to connect longitudinally, while the erosion zones are divided and restricted to the areas near both side-walls. At $T=43'$, the deposition zone in the central region enlarged and its height begins to exceed 0.5 cm, reducing widths of the erosion zone. Such a state of the bed variation becomes most distinctive at $T=66'$. Thus, in accordance with the alternate bar development, the erosion zones are limited to discrete regions near the side-walls being narrowed despite being deepened, while the eroded sediment is transported and deposited widely on the central region.

The bed variation narrowing the deep erosion zone remains as a hysteresis so that the alternate bars develop easily though they migrate downstream filling again the erosion zone, for such bed topography reduces the amount of sediment transport necessary for the bar advancing. In contrast, in an upstream reach, the amount of bed variation is almost the same as that in the early stage. It suggests, as aforementioned, that the upstream reach maintains the early state of the development process all the time under a uniform and steady sand supply condition.

4.2 Characteristic sediment transport in the development process of the alternate bar

As seen in **4.1**, the sediment transport in the development process is characterized by a lateral sediment movement from the erosion zone near the both side-walls to the central deposition zone. The sediment movement is caused by convergent and divergent currents over the developing bar corresponding to its topography, and it is illustrated schematically in **Fig. 15(a)**. That is to say more precisely, the sediment which is eroded mainly from the bed facing the bar front near the side-wall is carried and spreads radially over the downstream bar. Some portion of the eroded sediment is spent to fill the downstream erosion zone and contributes to the bar migration. The other main portion settles in the central part after crossing over the bar edge and makes the edge protrude outward, thus narrowing the erosion zone. The bed scour near the side-wall proceeds balancing the amount of the deposit portion and at the same time the wave height increases by as much as this increase in the scour depth, because the increase in the elevation of the deposition zone is much smaller than that in the scour depth.

Cross sections of the bed elevation are, therefore, expected to present bell-shapes or Quonset-hut-shapes if the elevation profiles as shown in **Fig. 13** are averaged longitudinally in a reach including an even number of alternate bars. **Fig. 16** demonstrates, in fact, the averaged cross sections of the bell-shape. The elevation in the central zone is higher than the mean bed level depicting the deposit zone while both sides are much lower with narrow width. By the comparison of **Fig. 16** with the figures in chapter **3**, the bell-shape can be recognized and becomes distinguished at the

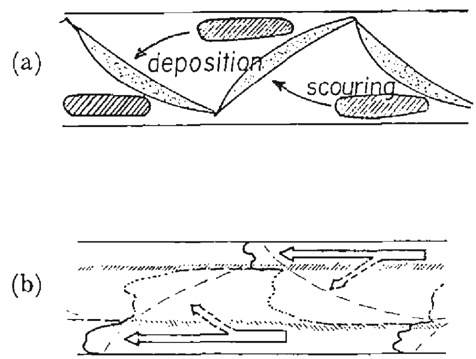

Fig. 15 A schematic sketch of the sediment movement in the development process (a) and that of the bed topography near the final state (b).

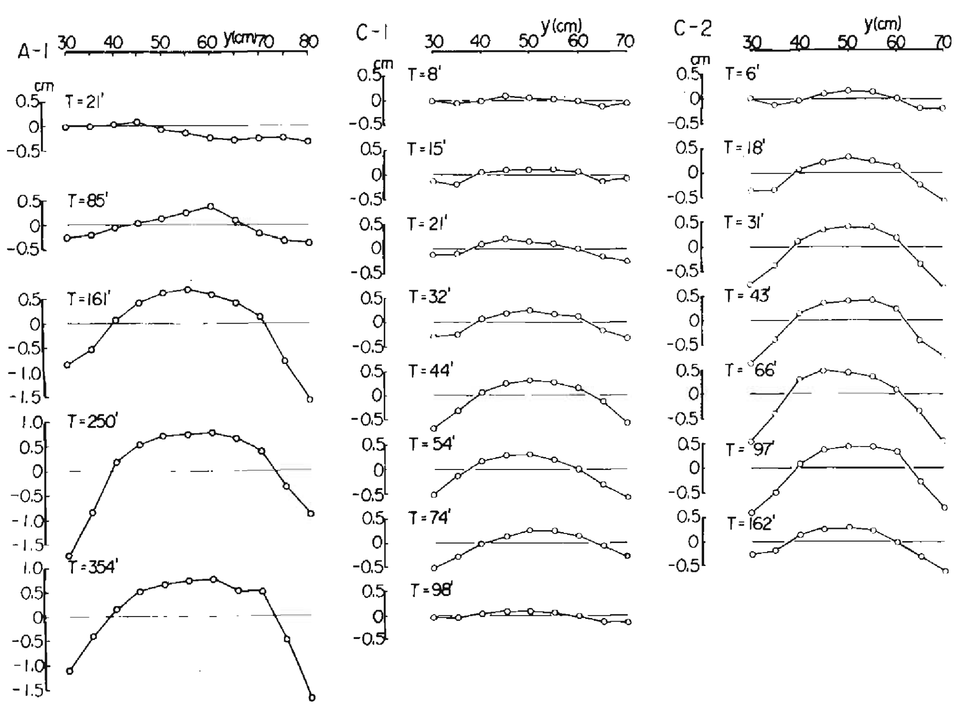

Fig. 16 Examples of bell-shaped cross section of the bed averaged longitudinally.

finish of the first phase of the development process, making itself clear and clear in the second phase. The height of the bell-shape, Z_K, is defined here as the difference between the maximum height in the central region and the minimum at either side. Z_K keeps increasing till $T=T_e$ similar to the wave height, Z_B, and after that decreases gradually because of the intrusion of new bars. The maximum values of Z_K at $T=T_e$ is noted as Z_{Ke}, and ratios of Z_{Ke} to Z_{Be} become as much as 0.5–0.7.

Thus, the formation of the bell-shaped cross sections express with fairly high fidelity the bed variation hysteresis which contributes to the bar development. The averaged sediment movement producing the bell-shaped cross section is worth inspecting to understand the comprehensive process of the bar development.

A mean lateral sediment transport rate per unit longitudinal distance, q_{By}, which forms the bell-shaped cross section, can be calculated from changes with time of the cross sections by using boundary conditions that $q_{By}=0$ at both side-walls. Then, a ratio, q_{By}/q_{Bx} is interpreted as a comprehensive direction of the sediment flux concerning the formation of the bell-shaped cross sections, where q_{Bx} is the longitudinal sediment load per unit width measured at the outlet. **Fig. 17** shows the variation of q_{By}/q_{Bx}, in which q_{By} is positive in the direction from the left side-wall to the right. Accordingly, in case of the uniform development, the curves of q_{By}/q_{Bx} delineate a point symmetrical Z-letter form: the positive sign of q_{By}/q_{Bx} turns to negative at the center corresponding to the sediment movement toward the central region and its absolute values at both sides are the same.

In run C–1, the curves are skewed to show an imbalance between the sediment fluxes in both directions during each flow duration, which suggests that bars facing to either the left or the right side-wall developed rapidly. But symmetrical curves seem to be obtainable in this case by using twice the calculated intervals, as the distortion of the curves appears in both sides by turns. In run C–2, the curves depict typically symmetrical forms till $T=31'$ in accordance with the uniform development observed. The curves are, however, distorted near $T_e(T=66')$, implying difficulties in maintaining uniform development, and the amplitudes of the curves become smaller showing decrease in the lateral sediment movement. Such variation of the curves is recognized most clearly and typically in run H–2, where the amplitudes of very regular curves increase corresponding to the accelerative bar growth during the former half of the second phase and after a while they decrease approaching the equilibrium state. As for runs D, variations of the curve before $T=100'$, when the distortion in the initial bed influenced the bed variation, must be left out of the consideration. The curves concerning the development appeared after $T=99'$ in run D–1, and after $T=132'$ in run D–2. The amplitudes then increased rapidly. Coming up to the finish of the second phase at $T=270'$ in run D–1 and at $T=540'$ in run D–2, the curves reduced in amplitude or left the sign unchanged.

Fig. 18 describes the variations of an intensity index of the lateral sediment transport, $\hat{q}_{By}/q_{Bx}$, defined by the difference between the maximum and minimum values of the q_{By}/q_{Bx} curves with changing sign from positive to negative. Referring to **Fig. 8**, the intensity indices also are seen to have peak values immediately after the finish of the first phase, and then decrease gradually to the equilibrium. In run C–2, the

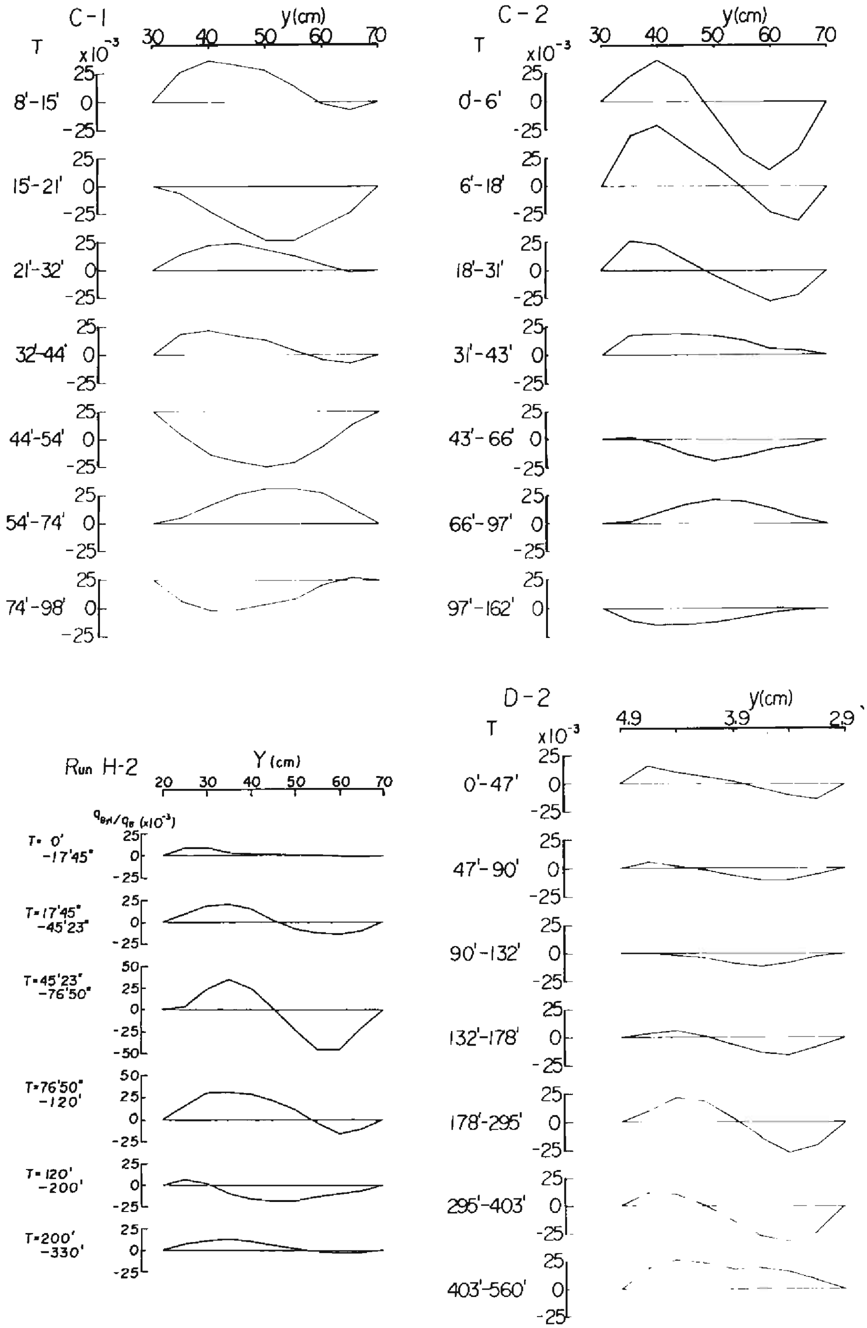

Fig. 17 Changes of averaged direction of sediment movement, q_{By}/q_{Bx}, in the development process.

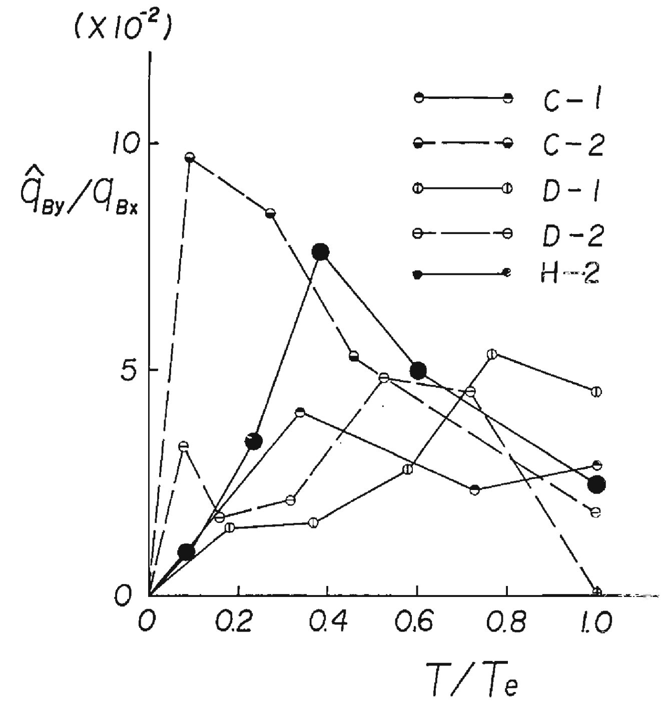

Fig. 18 Changes of intensity indeces of lateral sediment transport contributing to the alternate bar development.

first phase is regarded to finish in a very short time due to the influence of the initial bed condition. Though the peak values in runs C–2 and H–2 are a little larger than the others, the mean values during the development time are almost same. It is, therefore, pointed out that the state of the sediment movement to produce the alternate bar is very similar in runs C, D and H, inspite of the great difference in the experimental scales.

As indicated in chapter **3**, the first phase of the formative process of the alternate bar is affected seriously by the initial bed condition and differs much in each case. The detailed process of the first phase has been investigated[18]. From the results found out here, the second phase has several characteristic features common to the formative process under various conditions. In addition, the alternate bar grows greatly during the second phase. The mechanism of the alternate bar development in the second phase is summarized in the following section.

4.3 The machanism of the alternate bar development

The results obtained in the preceding sections conclude that the mechanism of the alternate bar development can be represented by that occurring in the second phase. Based on the results and introducing the flow characteristics over the alternate bar clarified already[15], the mechanism is summarized as follows:

(1) Meandering flow with convergence and divergence of the currents are caused by the oblique abrupt drops[16] at the bar edges which become distinctive and are arranged regularly after the first phase finished. According to such flow, bed scour occurs near the side-wall immediately downstream of the bar edge and some portion of the eroded sand moves toward the central region to deposit near the next bar edge.

(2) The growth of the wave height due to the lateral sediment transport makes the flow meandering more prominent which accelerates the increase in the wave height, and at the same time developing rate of the bell-shaped cross section takes the maximum value.

(3) This indicates the existence of a suppressing factor of the development since the wave height is observed to have a maximum value. It is reasonable to assume first that the suppressing factor is a lateral component of the gravity acting toward both side-walls from the center which is induced by the lateral slope of the Quonset-hut shaped bed. In addition, it is regarded as the second factor that the bed topography with Quonset-hut averaged shape weakens the meandering flow characteristics over the alternate bar, as mentioned below.

(4) It is mainly the gravitational supressing factor which reduces the sediment transport contributing to the bar growth. The wave height is considered to finish its development when the gravitational outward force balances the drag inward force.

Moreover, in the experiments, as shown schematically in **Fig. 15(b)**, it is often observed that the channel bed clearly become Quonset-hut shape with the flow split as if into two streams, making the bar edge obscure because of a very shallow current in the central region while the bar front edge is lowered with avalanching into the deeply scoured zone of the bar in the downstream reach. In such a case, the lateral component of the drag force disappears to move the sediment inversely toward both side-walls from the central region, decreasing the wave height as well as the bell-shaped height. New bars hardly form and develop till the bed is much flattened. Besides, even in cases when the flow is not divided completely, the meandering flow is possibly weakened to decrease the wave height slightly after the development of the Quonset-hut shaped bed, damping of which increases the wave height again. Either way, the alternate bar is presumed to repeat increase and decrease in the wave height even under steady flow conditions.

Formulating the mechanism above-mentioned, the development process can be predicted and, in fact, an estimation of the wave height and the wave length has been investigated already[11,12]. However, only the development time will be considered in the next section and effects of submerged parallel works of groynes, which supress the lateral components of both flow and sedimdnt transport, will be examined as an application problem in the next chapter.

4.4 A prediction of the development time

From the standpoint of the comprehensive bed variation, the development process of the alternate bar is regarded as the formation of the Quonset-hut shaped bed and almost all the development time is usually spent during its formation. The averaged sediment transport direction concerning its formation, $\hat{q}_{By}/q_{Bx}$, has nearly the same values and the variations, regardless of the channel size. The bell-shaped average cross sections also show very similar forms. According to these features, a prediction of the development time is tried as follows:

The bell-shaped cross sections are delineated schematically as in **Fig. 19** and the coordinates y and z are normalized by the width B and the height of the bell-shape Z_{Ke}, respectively. The forms of the averaged cross sections can be expressed by an equation because of their high similarity seen in **Fig. 16**,

$$z/Z_{Ke}=\mathrm{fn}(y/B). \tag{4}$$

Z_{Ke} is proportional to Z_{Be} and their ratio α_Z is about 1/2 from the results in the preceding secions.

$$Z_{Ke}=\alpha_Z Z_{Be}. \tag{5}$$

An area shown by shading in **Fig. 19**, A_K, indicates an amount of the sediment transport during the formation of the average cross section. The area A_K is reduced as

$$A_K=\alpha_A B Z_{Ke}=\alpha_A \alpha_Z B Z_{Be}, \tag{6}$$

where coefficient α_A is probably 0.3 from **Fig. 16**. The development time is considered to be proportional to a time when the area A_K is divided by the mean rate of the lateral sediment transport, q_{By}, where α_q is the mean value of $\hat{q}_{By}/q_{Bx}$ in the development time and can be regarded as a constant of about 5×10^{-2}. For the bell-shaped cross section is formed from both sides,

$$T_e=\alpha_t A_K/q_{By}=(\alpha_t \alpha_A \alpha_Z/\alpha_q)(BZ_{Be}/q_{Bx}), \tag{7}$$

where α_t is a proportional coefficient of nearly unity. Moreover, a definite proportional relation is known between the wave length of the alterante bar and the channel width, and its proportional coefficient α_l is approximately 5. By using α_l, eq. (7) yields

$$T_e=\alpha_T(l_{Be}Z_{Be}/q_{Bx}), \tag{8}$$

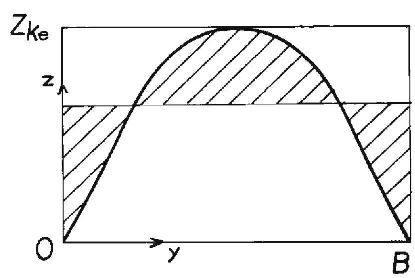

Fig. 19 A schematic sketch of the bell-shaped average cross section.

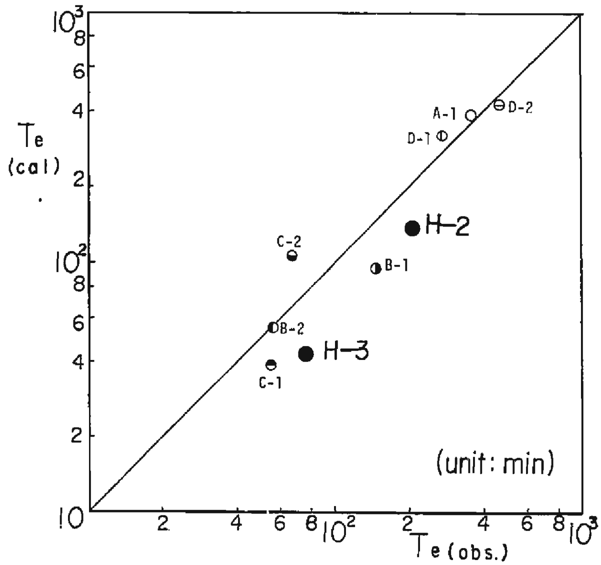

Fig. 20 The predicted development time of the alternate bar compared with the observed one.

where $\alpha_T=(\alpha_t\alpha_A\alpha_Z)/(\alpha_q\alpha_l)$. The expression in which l_{Be} is used instead of B has some possibility to include more or less the time required in the first phase.

Fig. 20 presents the relation between observed T_e and those calculated from eq. (8) and shows a definite proportional relation. In **Fig. 20**, the coefficient of proportion of 0.57 is used as a best fit and agrees very well with that calculated from the constants included in α_T, that is $\alpha_T=0.6$, indicating a high validity of the above derivation. The expression for the prediction of the development time can be applied widely since the shapes of the alternate bars of various scales is quite similar both longitudinally and laterally to each other.

Equation (8) has the same form as that for the development time of dunes proposed by Yalin[17]. But the derivation here is definitely based on mechanics considerations. On the other hand, it must be said that Yalin's explanation deriving the equation is quite obscure, especially on the sediment movement to form dunes.

5. Effects of submerged parallel groyne works on the alternate bar

5.1 Control of the alternate bar

Control of the alternate bar might have been tried since relatively early days in European countries for the purpose of the maintenance of navigation channels. In our country, several types of river regulating works were introduced into the Yodo river, the Kiso river and so on. However, use of these works were restricted to the individual rivers with some distinguished features, and few systematic studies have been carried out on the control of the alternate bar by grasping the hydraulic characteristics of the bar. For example, Sasaki[17] carried out experiments with various kind of groynes for the prevention of flow meandering in low water courses. But consistent description of effects of the groynes was difficult to present because of a lack of information on the bar characteristics. Kinoshita and Miwa[18,19] investigated the control of the migration of the alternate bars, conducting systematic experiments in zigzag channels and in channels with bed fixing works, the top planes of which were inclined alternately. They clarified that the migration stops when the intersection angle of the channel segments exceeds 20° and a similar effect appears in the latter case with bed fixing works.

In contrast, control of the bar geometry has scarcely been tried. The results in chapter **4** give some suggestion on controlling the bar geometry. The wave height of the alternate bar is developed and preserved by the lateral sediment movement due to the lateral velocity component induced by the oblique bar edge. Accordingly, if the lateral component of the sediment movement is weakened, the alternate bar will fail to maintain the wave height changing the geometry. The lateral component becomes very weak when the channel is split into two channels, and it is practically impossible. But sediment transport may also be controlled by relatively small scale works such as submerged groyne works because it occurs immediately above the channel bed. Considering the observations of the flow conditions forming the alternate bar, the flow condition seems able to be changed remarkably by a certain kind of small irregularlities, and the submerged groyne works may vary the flow condition greatly. Parallel works are regarded most suitable as the type of such groyne works for application to traveling alternate bars. Such regulating works based on the control of the lateral components of both flow and sediment load have a similar aspect to the so-called Iowa vanes proposed recently by Odgaard and Kennedy[20] as bank protection works in river bends.

Thus, experiments were carried out in two cases where parallel works were laid continuously and intermittently on the developed alternate bar bed.

5.2 Experiments with submerged parallel works on the alternate bar bed

Experiments were conducted in accordance with run C–2: after the experimental conditions were prescribed the same as in run C–2, alternate bars were developed in a 60′ flow duration with sand supply. Then, pieces of plywood 4 cm in height and 12 mm in thickness were buried continuously or intermittently as the parallel works along the centerline in a reach with developed alternate bars. Differences between the top of the works and the bed surface are a maximum of 5 mm and a minimum of 2 mm. Sand grains overtopping the works was indiscernible. Intermittent works were produced by laying four 1.6 m long blocks with 0.8 m spacings in a 8.8 m reach upstream from the outlet. After the laying of the works, the flow began again and the effects of the works were observed and photographically recorded. In addition, in the case of intermittent works, the wave length and the wave height were measured before and after the works were introduced.

Fig. 21 shows the effects of the submerged intermittent parallel works, in which $T=0'$ at the beginning of the second flow. Sand grains were hardly carried over the centerline as well as the groynes and the state of the sediment movement was divided into two courses as if two channels of a half width were arranged side by side. In this case, filling up of the thalweg was mostly completed by $T=32'$ and new small bars formed corresponding to the half width at $T=42'$. The geometry of the bars before the laying of works and at $T=42'$ are compared in **Table 4**. Both the wave length and the height were reduced at $T=42'$ to one third of those before the laying, indicating a remarkable effect of the parallel works on the bar geometry. It is, however, necessary to pay attention to the local scour around the upstream end of each groyne block.

In case of the submerged continuous parallel works, the state of the sediment movement was split completely and the alternate bars turned clearly into those corresponding to the half width. The effects of the continuous parallel works were much more prominent than that of the intermittent works.

As mentioned above, the submerged parallel works, even laid intermittently,

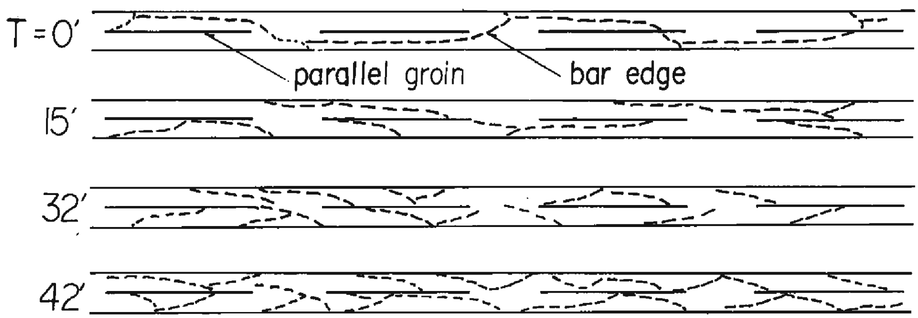

Fig. 21 Deformation of the alternate bars due to the submerged parallel groyne works laid intermittently.

Table 4 Effect of the submerged parallel groyne works laid intermittently.

Time		Geometry of individual bars					Mean value
$T=0'$	l_B (m)	2.48	1.87	2.53	1.30	1.25	1.89
	Z_B (cm)	1.80	2.65	3.00	2.60	1.85	2.38
$T=42'$ left	l_B (m)	0.63	0.68				0.66
	Z_B (cm)	0.75	0.60				0.68
right	l_B (m)	0.63	0.80	0.89	0.56		0.69
	Z_B (cm)	0.75	1.05	0.70	0.45		0.72

can change the sediment transport condition as if divided into two channels and can control the bar geometry. Large effectiveness may be expected when the parallel works will be applied to the river course impeded by developed alternate bars. Furthermore, the results here suggest the same effectiveness of the parallel works if introduced in braided streams.

6. Conclusion

The alternate bar plays one of major roles in stream channel processes and has a large influence on the safety of the river course and various uses of the river water. The process and the mechanism of the alternate bar development are investigated in this paper, which is regarded as one of the most important subjects on the meso scale river bed configuration, considering the present circumstances of the studies. Conducting the experiments under widely changing conditions, particularlly that of the channel width, we clarified the characteristic changes of the wave length and the wave height of the alternate bar and the channel bed variations in the development process in detail. By using the results, we proposed an equation for the development time of the alternate bar, and moreover, experimentally verified an effectiveness of parallel groyne works for the control of the bar geometry. The results of this investigation are summarized as follows:

(1) The formation of the alternate bar is observed usually to propagate downstream rather quickly from a prominent bar which developed rapidly and the wavelength are, therefore, prolonged with time. The increase in the wave length is rapid in the early stage. Such a process differs from the premises of the stability theories which assume uniform progress of bar formation with constant wave length.

(2) The wave length is determined rather rapidly after the propagation of the bar edge formation and then the wave height increases greatly till the bar geometry reaches an equilibrium state. Accordingly, the development process is divided into three phases: in the first phase, the bar edge becomes distinctive and the wave length approaches almost to the equilibrium value. In the second, the growth of the wave height is predominant and in the third, both the wave length and the wave height slightly fluctuate near the equilibrium values.

(3) The finish of the second phase is defined reasonablely as the time when the wave height takes the first maximum value and the time required to reach this point is also defined as the development time of the alternate bar, the large portion of which is spent in the second phase in the usual case. On contrast, the duration of the first phase is varied according to the initial bed and the upstream end conditions. A nondimensionalized wave height by the grain size is proportional to 2/3 power of a ratio of the width to grain size at the finish of the first phase defined tentatively as the time when the wave length becomes 60% of the equilibrium value.

(4) The wave height is increased by the lateral sediment movement from both

sides to the central part due to the flow over the oblique bar edge. At the same time, the channel bed becomes Quonset-hut shaped with the bell-shaped average cross section. The formation of this shape represents the whole development process.

(5) The lateral component of the sediment load calculated from the change of the bell-shaped cross section shows a fairly similar variation and has a relatively constant rate to the longitudinal one, regardless of the channel scales. By using the results, a equation estimating the development time is derivated definitely and the predicted values show a good agreement with the observed ones.

(6) The submerged parallel groyne works, buried either continuously or intermittently in a bed with developed alternate bars, were found through experimental examinations to have a great effectiveness for bar geometry control.

As summarized above, the most essential mechanism of the development process of the alternate bar was clarified comprehensively to give the bases for the prediction of bar behavior under varying flow conditions and for the verification of the premises in the stability theories. We have already tried to express the mechanism described qualitalively by using the basic equations of sediment hydraulics for the quantitative analyses of the process. Simultaneously, we have carried out experiments on the first phase of the development process and have accumulated fundamental informations on the formation of the bar edges and the process after that[13]. We will present these results in the near future.

Acknoledgement

We express our gratitude to Mr. Shuji Horiike, Mr. Tsuyoshi Koike and Mr. Takashi Furukawa, who were graduate students at that time. They collaborated with us ardently to carry out the experiments and to analyse the results. This investigation would not have been accomplished without their powerful support. We thank Mr. Yukio Nakamura, the technical officer of the Research Section for River Disaster Prevention, for his aid in the execution of the experiments and the drawing up of diagrams in this paper. We are grateful to the staffs of the workshop of the Ujigawa Hydraulic Laboratory for their support to mannufacture the experimental apparatus. We are glad to have had comments on the manuscript from Prof. Gary Parker of the University of Minnesota.

References

1) Muramoto, Y. and Y. Fujita: A classification and formative conditions of river bed configuration of meso scale, Proc., the 22nd Japanese Conf. on hydraulics, 1978, pp. 275–282 (in Japanese).

2) Fredsøe, J.: Meandering and braiding of rivers, J. Fluid Mech., Vol. 76, Part 3, 1976.

3) Kuroki, M. and T. Kishi: Study on regime criteria of river morphology, Proc., the 26th Japanese Conf. on hydraulics, 1982, pp. 51–56 (in Japanese).

4) Engels, H.: Untersuchungen über die Bettausbildung gerader oder schwach gekrummter Flussstrecken mit beweglicher Sohle, Zeitschrift fur Bauwesen, 1905. (cited from Sukegawa, N:

Hydraulic studies on flow meandering phenomena in straight river channels, Research material, Bureau of Resources, Science and Technology Agency, 1971, pp. 40–41.)

5) Kinoshita, R.: Research studies on stream channel metamorphosis of the river Ishikari —Trunk edition—, Research material, Bureau of Resources, Science and Technology Agency, No. 36, 1962, pp. 88–91 (in Japanese).

6) Ikeda, H.: Alternate bars in experimental flumes and their formative conditions, Chirigaku Hyoron (J. Geography), 46–7, 1973, pp. 435–451 (in Japanese).

7) Kondou, Y. and H. Komori: Fundamental experiments on alternate bars, Monthly Rep., Experimental Station on Public Works, Hokkaido Development Bureau, No. 251, 1974.

8) Muramoto, Y. and Y. Fujita: Study on meso-scale river bed configuration, Annuals, Disast. Prev. Res. Inst., Kyoto Univ., No. 20B–2, 1977, pp. 243–258 (in Japanese).

9) Fukuoka, S., T. Nakamura, K. Abe and T. Igarashi: Hydraulic roles of side banks in alluvial streams, Proc., the 27th Japanese Conf. on Hydraulics, 1983, pp. 681–688 (in Japanese).

10) Fujita, Y., Y. Muramoto and S. Horiike: Study on the process of alternating bar development, Annuals, Disast. Prev. Res. Inst., Kyoto Univ., No. 24B–2, 1981, pp. 411–431 (in Japanese).

11) Fujita, Y., Y. Muramoto, S. Horiike and T. Koike: On the mechanisms of alternating bar development, Proc., the 26th Japanese Conf. on hydraulics, 1982, pp. 25–30 (in Japanese).

12) Fujita, Y., T. Koike and Y. Muramoto: The mechanism of wave length development of alternate bars, Proc., the 29th Japanese Conf. on Hydraulics, 1985, pp. 485–490 (in Japanese).

13) Fujita, Y., T. Koike, T. Furukawa and Y. Muramoto: Experiments on the initial stage of alternate bar formation, Annuals, Disast. Prev. Res. Inst., No. 28B–2, 1985 (in Japanese, in Press).

14) Fujita, Y. and Y. Muramoto: Experimental study on stream channel processes in alluvial rivers, Bull., Disast. Prev. Res. Inst., Kyoto Univ., Vol. 32, Part. 1, 1982, pp. 49–96.

15) Fujita, Y.: Experimental study on the flow characteristics over alternating bars, Proc., the 24th Japanese Conf. on Hydraulics, 1980, pp. 329–337 (in Japanese).

16) Muramoto, Y. and Y. Fujita: Experimental study on the flow over abrupt drop with oblique edge, Annuals, Disast. Prev. Res. Inst., Kyoto Univ., No. 21B–2, 1978, pp. 277–291 (in Japanese).

17) Yalin, M.S.: On the development of sand waves in time, Proc., the XVIth Congress, IAHR, Sao Paulo, Brazil, Vol. II, 1975, pp. 212–219.

18) Sasaki, H.: Studies on the rationalization of the river course design, Doctral thesis presented to Kyoto Univ., 1968 (in Japanese).

19) Kinoshita, R. and H. Miwa: Planform of stream channel stabilizing the alternate bar location, Shin-Sabo, Vol. 94, 1974 (in Japanese).

20) Miwa, H.: On the stabilization of thalwegs by series of alternately inclined bed fixing works, Proc., Annual Meeting of Japan Society of Agricultural engineers, 1978 (in Japanese).

21) Odgaard, A.J. and J.F. Kennedy: River bend bank protection by submerged vanes, Proc., ASCE. J. Hydraulic Div., Vol. 109, HY8, 1983, pp. 1161–1173.